IN SILICO ANALYSIS OF DIFFERENTIAL BINDINGS BETWEEN MULTIPLE ISOFORMS OF USP21 AND YOD1 TO PREDICT THEIR EFFECTS ON LUNG CANCER

Bioresearch Communications
Volume 12, Issue 2, July 2026

DOI:
doi.org/10.3329/brc.v12i2.91520

Ahadul Islam Fahim, Md. Hasib#*, Rehana Parvin#*, Tasnim Hossain Tanha, Shaila Haque, Fahmida Sultana Rima and Ziasmin Khatun

Department of Biochemistry and Biotechnology, University of Barishal, Barishal-8254.

#These authors contributed equally to this research

ABSTRACT

The Hippo signaling pathway plays an important role in human diseases. This pathway takes part in the initiation, development and metastasis of various types of cancers, including lung cancer. The effector molecules of this pathway, Yes-associated protein 1 (YAP), Tafazzin (TAZ), undergo constant regulation. In the cytoplasm, YAP/TAZ are degraded in multiple ways, the ubiquitin-dependent degradation being the most prominent one. Ubiquitin specific proteases 21 (USP21) and YOD1 are two of the many deubiquitinating enzymes that participate in the regulation of ubiquitination on YAP/TAZ. Although the roles of USP21 and YOD1 vary from disease to disease, they have a tumor suppressing role in lung cancer. These two enzymes also interact to stabilize each other and show a synergistic effect in inhibiting cell proliferation in lung cancer. Therefore, this study was designed to predict which set of isoforms of USP21 and YOD1 shows stable interactions and how it could affect lung cancer. Using a number of *in silico* techniques such as protein structure prediction, structure validation, docking analysis and molecular dynamics simulation studies, it was identified that the USP21 isoform b and YOD1 isoform 1 show the most stable interaction. Thus, it was predicted that these set of isoforms would exhibit better suppression of lung cancer.

KEYWORDS: Hippo-signaling-pathway, lung-cancer, deubiquitinating-enzyme, molecular dynamics simulation, USP 21, YOD1

RECEIVED: 30 May 2026, ACCEPTED: 25 June 2026

TYPE: Original Article

***CORRESPONDING AUTHORS: Dr. Rehana Parvin & Md. Hasib, Department of Biochemistry and Biotechnology, University of Barishal, Barishal-8254.**
Email: rehanadu@yahoo.com; hsbharic22@gmail.com

Introduction

Ever since its discovery some 20 years ago in *Drosophila melanogaster*, the Hippo signaling pathway has been studied extensively because of its pivotal role in the development and homeostasis of organs. The pathway consists of many key components, including the mammalian STE20-like kinase 1/2 (MST1/2), MOBKL1A/B (MOB1A/B), protein Salvador homologue (SAV1), Yes-associated protein 1 (YAP), Tafazzin (TAZ), large tumor suppressor kinase 1/2 (LATS1/2) and the transcriptional enhanced associated domain (TEAD) family (Cheng *et al.*, 2020). YAP/TAZ regulate gene expression by interacting with TEAD1-4 transcriptional factors, thereby controlling cell proliferation, differentiation, stem cell self-renewal and apoptosis (Kwon *et al.*, 2013). Using the C-terminal SARAH (Sav/Rassf/Hpo) domains, MST1/2 interacts with SAV1 to phosphorylate LATS1/2 kinase, MOB1 and SAV1 (Chan *et al.*, 2005; Hergovich *et al.*, 2006; Praskova *et al.*, 2008). YAP and TAZ are directly phosphorylated at multiple sites by LATS1/2, which inhibits the nuclear localization of these proteins (Huang *et al.*, 2005; Zhao *et al.*, 2007). Subsequently, these phosphorylated YAP/TAZ proteins bind to 14-3-3 and their localization is sequestered in the cytoplasm, which leads to YAP/TAZ inhibition. Moreover, phosphorylation by casein kinase 1 results in the β-TrCP-mediated ubiquitination and proteasomal degradation of YAP/TAZ proteins (Liu *et al.*, 2010; Zhao *et al.*, 2007, 2010).

Dysregulation of the Hippo pathways is a hallmark of numerous cancers. MST1/2 and LATS1/2 function as tumor suppressors, whereas YAP/TAZ were reported as oncoproteins(Hall *et al.*, 2010; Liu *et al.*, 2010; Lu *et al.*, 2010; Xia *et al.*, 2002; Zhao *et al.*, 2007, 2010; Zhou *et al.*, 2009). Therefore, Hippo pathway dysregulation can lead to severe diseases, including cardiac disease(Austin *et al.*, 2019; Wang, Liu, *et al.*, 2018), eye disease(Lee *et al.*, 2018; Zhu *et al.*, 2018), pulmonary disease (Chanda *et al.*, 2019), hepatic disease(Driskill and Pan, 2021; Russell and Camargo, 2022), renal disease (Bergmann *et al.*, 2018; Ma and Guan, 2018) and immune dysfunction(Hong *et al.*, 2018; Zhang *et al.*, 2018). Studies have also identified that the MST1/2, LATS1/2, YAP and TAZ, the four main component of the Hippo signaling pathway takes part in the development of chemotherapy resistance (Zeng and Dong, 2021). YAP nuclear localization or overexpression of YAP and TAZ decrease the efficacy of doxorubicin, cisplatin, Taxol and 5-fluoracil, while downregulation of MST1/2 and LATS1/2

develop resistance to 5-fluoracil and cisplatin (Qin *et al.*, 2020; Ren *et al.*, 2008; Touil *et al.*, 2014; Wang, Sun, *et al.*, 2018; Wu *et al.*, 2021; Yao *et al.*, 2019; Zhang *et al.*, 2011).

Ubiquitin enzyme marks proteins to alter their function or degradation (Chen and Sun, 2009) whereas the deubiquitinating of enzymes remove the ubiquitin from proteins, resulting in their rescue from degradation. Approximately, 100 deubiquitinases (DUBs) have been identified (Nijman *et al.*, 2005) with the ubiquitin specific proteases (USPs) are the largest family of deubiquitinating enzyme. Among them, ubiquitin specific proteases 21 (USP21) involved in regulating cellular homeostasis and cancer. USP21 overexpression regulate the stability of MARK-1, -2 and -4, suppressing the transcriptional activity of YAP (Nguyen *et al.*, 2017), which indicated that MARKs act as interacting partners of USP21. Furthermore, a recent study provides other contradictory evidence that USP21 interacts with and stabilizes forkhead box protein M1 (FoxM1), a transcription factor, to enhance the nuclear translocation and transcriptional activity of YAP. As previously described by Sun et al., FoxM1 inhibit YAP phosphorylation to promote nuclear translocation and transcriptional activity of YAP (Li *et al.*, 2022); however, the underlying mechanism requires further study (Sun *et al.*, 2020). Taken together, the discrepancies in USP21 modulation of the Hippo signaling pathway may be explained by differences in cell context-specific regulation.

The OTU deubiquitinases subfamily contains 16 members in humans, and these enzymes have been implicated in numerous human diseases such as cancer, neurodegeneration, inflammation, and virus infection (Clague *et al.*, 2012). In *Drosophila melanogaster*, The OTU domain was first identified in an ovarian tumor gene by bioinformatics analysis (Makarova *et al.*, 2000). The Otu gene product participates in the division and differentiation of the cystoblast cell (Rodesch *et al.*, 1995; Sass *et al.*, 1995). Studies have revealed that some OTU family members are deubiquitinating enzymes containing putative catalytic histidine and cysteine residues (Balakirev *et al.*, 2003; Reyes-Turcu *et al.*, 2009). YOD1, also known as OTUD2, possess the ability to remove conjugated ubiquitin from substrates and take part in endoplasmic reticulum-associated degradation (ERAD) of misfolded proteins (Ernst *et al.*, 2009). YOD1 harbors the essential catalytic DUB activity, but also use its S2 ubiquitin binding site to function as a ubiquitin sensor. Ubiquitin binding by YOD1 stimulates the interaction of YOD1 with p97, in turn, p97 activates ubiquitin binding of YOD1. YOD1 plays a role in regulation of macroautophagy, including the clearance of damaged lysosome by recruiting UBXN6 (UBX domain-containing protein 6), PLAA (phospholipase A-2-activating protein), and VCP (valosin-containing protein) to damaged lysosome membranes (Papadopoulos *et al.*, 2017).

In the A549 cell line, there is conflicting research on the cellular functions of USP21. Nguyen et al. reported that YAP/TAZ activity and cell proliferation is increased due to knockdown of USP21 in A549 cells (Nguyen *et al.*, 2017). However, another study reported that deubiquitination and stabilization of Yin Yang-1 (YY1), an oncoprotein, by USP21 promotes non-small cell lung cancer (NSCLC) cell proliferation, migration, and invasion, including A549 cells (Xu *et al.*, 2020). YOD1 inhibits cell proliferation in A549 cells. Interestingly, greater inhibition of cell proliferation was found in co-transfection of Myc-*YOD1* and Flag-*USP21* as compared to transfection with Myc-*YOD1* or Flag-*USP21* alone. However, there are cell lines in which no synergistic effects of YOD1 and USP21 on cell proliferation was found. Compared to transfection with Myc-*YOD1* or Flag-*USP21* alone, co-transfection of Myc-*YOD1* and Flag*USP21* did not inhibit cell proliferation in HEK293T or HeLa cell. Increased expression of p-YAP was observed in A549 cells co-transfected with Myc-*YOD1* and Flag-*USP21* compared to transfection with either Myc-*YOD1* or Flag-*USP21* alone (Park and Baek, 2023). These findings suggest that the synergistic effect of YOD1 and USP21 can regulate the Hippo signaling pathway, which leads to the suppression of specific cancer cell proliferation. Therefore, this study employed various bioinformatics tools to identify the differential binding interactions among multiple isoforms of USP21 and YOD1 and to predict their effects on lung cancer through modulation of Hippo signaling pathway.

Materials and Methods

Sequence Retrieval

The amino acid sequences of the USP21 isoform a (accession no. NP_001306776.1), USP21 isoform b (accession no. NP_001306777.1), USP21 isoform c (accession no. NP_036607.3), YOD1 isoform 1 (accession no. KAI4084766.1) and YOD1 isoform 2 (accession no. KAI4084767.1) were retrieved from the National Center for Biotechnology Information (NCBI) (Sayers *et al.*, 2011).

Secondary and Tertiary Structure Prediction

The secondary structure of the selected proteins was predicted through the SIMPA96 toolkit (Gröhl *et al.*, 2022). The tertiary structure of the USP21 and YOD1 isoform protein sequences were predicted through the HHpred (Söding *et al.*, 2005) webtool of the MPI Bioinformatics toolkit server (Zimmermann *et al.*, 2018). HHpred is a fast server for detection of remote protein homology and structure prediction and pairwise comparison of profile hidden Markov models (HMMs) was first used by this server.

Refinement and Quality Assessment

The GalaxyRefine server was used for further refining the predicted structures (Heo *et al.*, 2013). The GalaxyRefine web server is based on a refinement method that has been successfully tested in CASP10. The structures with the best quality and performance were selected after analyzing all the potential structures generated through refinement. Evaluation of the 3D structure of the proteins was performed using PROCHECK and ERRAT modules of the SAVESv6.1 server (https://saves.mbi.ucla.edu/) and the QMEAN tool of the ExPASy server (https://www.expasy.org/) to estimate the QMEANDisCo score and quality of the predicted models (Benkert *et al.*, 2008; Colovos and Yeates, 1993; Laskowski *et al.*, 1993).

Docking Analysis

In order to identify the interactions of the USP21 isoforms with YOD1 isoforms, protein-protein docking analysis was performed using ClusPro and HADDOCK v2.4 tool and PRODIGY (Honorato *et al.*, 2024; Kozakov *et al.*, 2017; Xue *et al.*, 2016). ClusPro is the first web-based, completely automated application for protein structure computational docking. HADDOCK (High Ambiguity Driven protein-protein DOCKing) encodes information from identified or expected protein interfaces in ambiguous interaction restraints (AIRs), setting it apart from ab-initio docking approaches. The web services under PRODIGY (PROtein binDIng enerGY

prediction) are aimed at predicting binding affinity in biological complexes and identifying biological interfaces from crystallographic ones. The residue level protein-protein interaction was visualized through BIOVIA Discovery Studio Visualizer (Kemmish *et al.*, 2017).

Molecular Dynamics Simulation Study

The molecular dynamics simulations study was performed in the iMODS server. The collective functional motions of biological macromolecules are naturally reproduced by normal mode analysis (NMA) in internal (dihedral) coordinates. Even with massive macromolecules, iMODS makes it easier to explore such modes and creates workable transition paths between two homologous structures (López-Blanco *et al.*, 2014).

Results

Protein structure prediction and validation

The secondary structures of the selected USP21 and YOD1 isoforms were predicted using the SIMPA96 toolkit (**Table 1**). All isoforms showed a predominance of random coils, followed by α-helical regions, suggesting considerable structural flexibility. The three-dimensional models generated by HHpred were refined and subsequently evaluated using ERRAT, Ramachandran plot analysis, and QMEANDisCo scoring (**Table 2**). The validation results indicated acceptable model quality, supporting the use of these refined structures for subsequent docking and simulation analyses.

Table 1. Secondary structure of the selected proteins predicted by SIMPA96 toolkit.

Protein	Alpha Helix	Beta Turn	Random Coil
USP21 isoform a	146 (24.54%)	0 (0%)	387 (65.04%)
USP21 isoform b	141 (25.54%)	0 (0%)	359 (65.04%)
USP21 isoform c	141 (24.91%)	0 (0%)	366 (64.66%)
YOD1 isoform 1	75 (21.49%)	0 (0%)	198 (56.73%)
YOD1 isoform 2	74 (24.26%)	0 (0%)	158 (51.80%)

Table 2. Evaluation of the 3D structures of selected proteins.

Protein	ERRAT Quality Factor	Ramachandran Favored	QMEANDisCo
USP21 isoform a	85.1266	94.50%	0.81 ± 0.05
USP21 isoform b	92.4658	92.90%	0.80 ± 0.05
USP21 isoform c	87.6289	93.50%	0.81 ± 0.05
YOD1 isoform 1	90.2439	93.90%	0.65 ± 0.06
YOD1 isoform 2	90.9091	94.40%	0.64 ± 0.06

Molecular docking analysis

Protein-protein docking was performed using ClusPro and HADDOCK to evaluate the binding patterns among the selected USP21 and YOD1 isoforms, while PRODIGY was used to estimate the binding affinity of the docked complexes. The best-ranked docking poses from each platform were selected for further analysis based on their respective scoring criteria and visual inspection of the docked conformations (**Figures 1 and 2**). The docking scores and predicted binding affinities are summarized in Table 3. Among the evaluated complexes, USP21 isoform b-YOD1 isoform 1 showed the strongest predicted binding affinity in PRODIGY, with a ΔG value of -18.3 kcal/mol. Although ClusPro identified USP21 isoform b-YOD1 isoform 2 as the lowest-energy complex, the overall docking profile supported USP21 isoform b-YOD1 isoform 1 as a promising interaction pair for subsequent stability assessment.

Table 3. Docking analysis scores from ClusPro, HADDOCK and PRODIGY.

Docked Isoforms	Cluspro Lowest Energy Score	HADDOCK		PRODIGY
		Docking Score	Z-score	Binding Affinity ΔG (kcal mol^{-1})
USP21 isoform a and YOD1 isoform 1	-1253.1	-14.0 ± 11.6	-1.7	-17.7
USP21 isoform a and YOD1 isoform 2	-1098.5	27.4 ± 1.9	-1.3	-14.4
USP21 isoform b and YOD1 isoform 1	-1159.1	57.4 ± 55.5	-1.8	-18.3
USP21 isoform b and YOD1 isoform 2	-1321.7	29.8 ± 35.0	-1.5	-15.1
USP21 isoform c and YOD1 isoform 1	-1235.5	-6.5 ± 8.0	-1.9	-16.2
USP21 isoform c and YOD1 isoform 2	-1192.7	6.8 ± 24.9	-1.7	-15.0

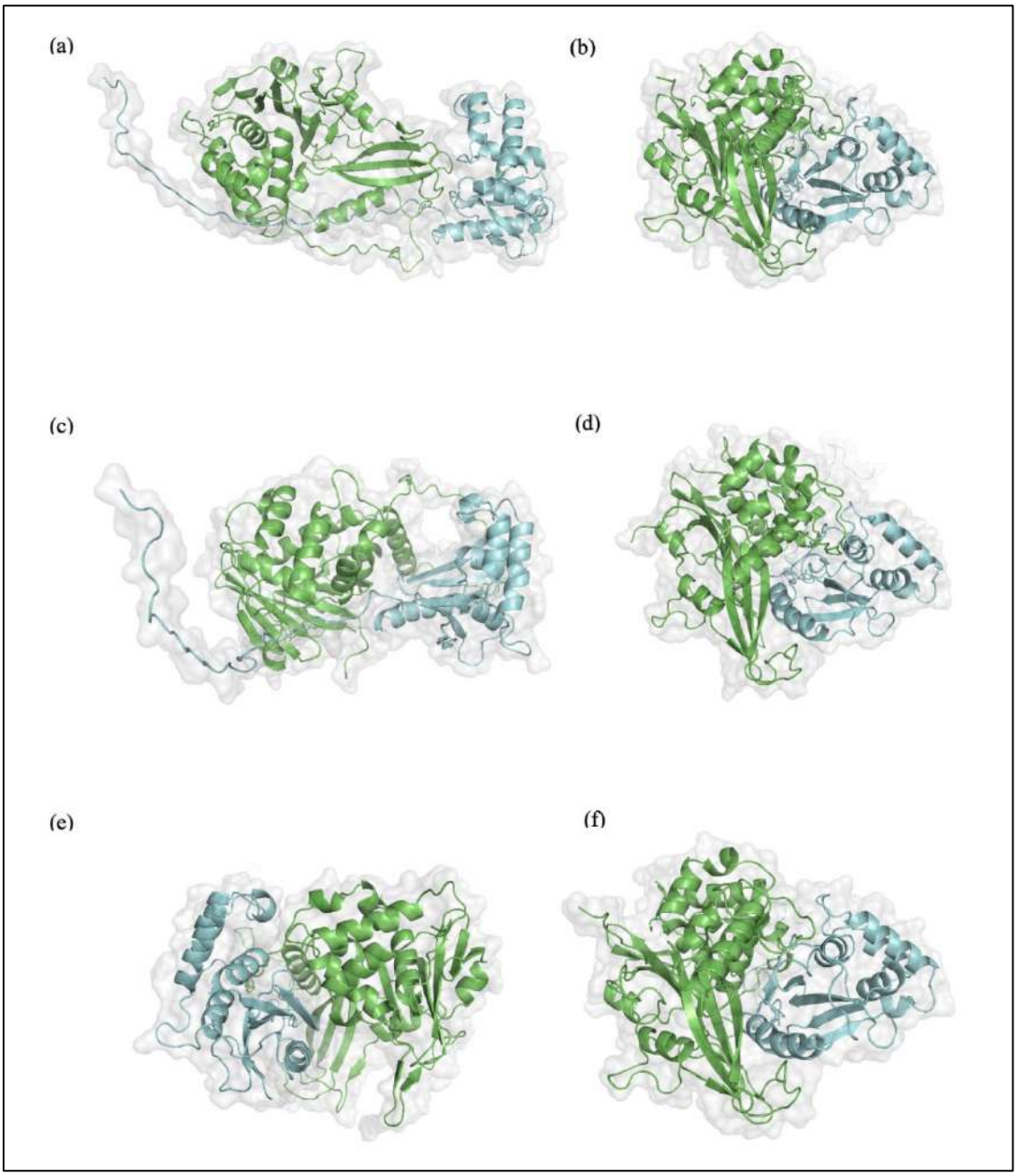

Figure 1. ClusPro server results of docking between (a) USP21 isoform a and YOD1 isoform 1 (b) USP21 isoform a and YOD1 isoform 2 (c) USP21 isoform b and YOD1 isoform 1 (d) USP21 isoform b and YOD1 isoform 2 (e) USP21 isoform c and YOD1 isoform 1 and (f) USP21 isoform c and YOD1 isoform 2.

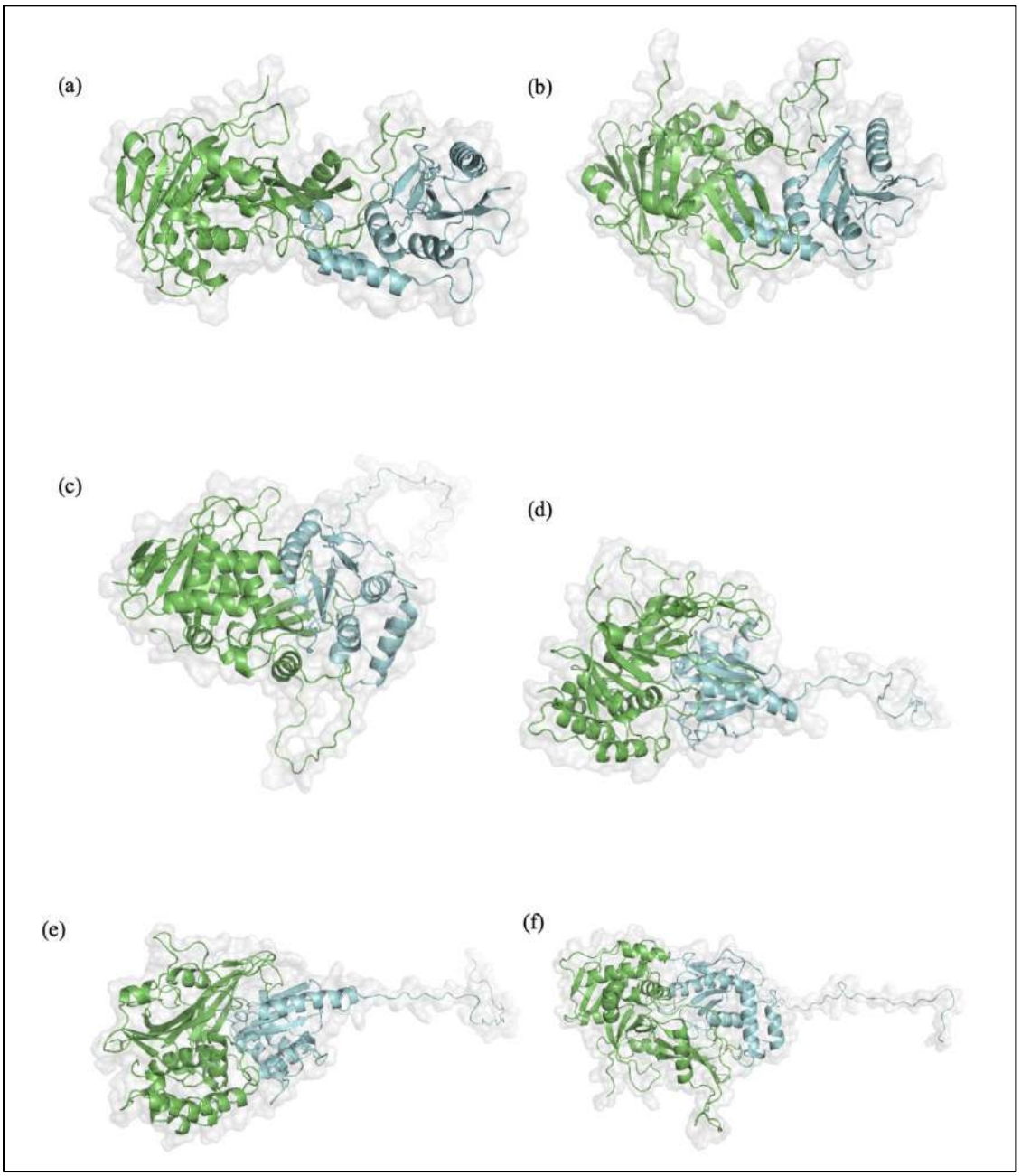

Figure 2. HADDOCK server results of docking between (a) USP21 isoform a and YOD1 isoform 1 (b) USP21 isoform a and YOD1 isoform 2 (c) USP21 isoform b and YOD1 isoform 1 (d) USP21 isoform b and YOD1 isoform 2 (e) USP21 isoform c and YOD1 isoform 1 and (f) USP21 isoform c and YOD1 isoform 2.

MD simulation results

The dynamic stability and flexibility of the docked USP21-YOD1 complexes were evaluated using the iMODS server based on normal mode analysis. To compare the stability of complexes generated by two independent docking platforms, iMODS analysis was performed separately for the HADDOCK-derived docked complexes and the ClusPro-derived docked complexes. The results obtained from HADDOCK docking are presented in Figures 3-7, whereas the corresponding results obtained from ClusPro docking are shown in Figures 8-12.

For each docked complex, five major parameters were analyzed: deformability, B-factor, eigenvalue, covariance matrix, and elastic network model. The deformability plot was used to identify flexible regions within the complexes, where higher peaks indicate residues with greater mobility and potential hinge regions. The B-factor plot reflected the relative atomic mobility predicted by normal mode analysis. The eigenvalue represented the stiffness of each complex, with higher eigenvalues indicating greater resistance to deformation and comparatively higher structural stability. The covariance matrix was used to assess correlated, anti-correlated, and uncorrelated motions among residue pairs, represented by red, blue, and white regions, respectively. Finally, the elastic network model illustrated the connectivity and spring stiffness

among atom pairs, where darker regions indicate stronger interactions and a more rigid structural network.

For the HADDOCK-derived complexes, the deformability, B-factor, eigenvalue, covariance matrix, and elastic network profiles are shown in Figures 3, 4, 5, 6, and 7, respectively. These analyses provided an overview of the flexibility and internal motion patterns of the HADDOCK-generated USP21-YOD1 complexes. Similarly, the ClusPro-derived complexes were analyzed using the same iMODS parameters, with deformability, B-factor, eigenvalue, covariance matrix, and elastic network model presented in Figures 8, 9, 10, 11, and 12, respectively. The use of both HADDOCK- and ClusPro-derived complexes allowed comparative assessment of the predicted structural stability of USP21 and YOD1 isoform interactions.

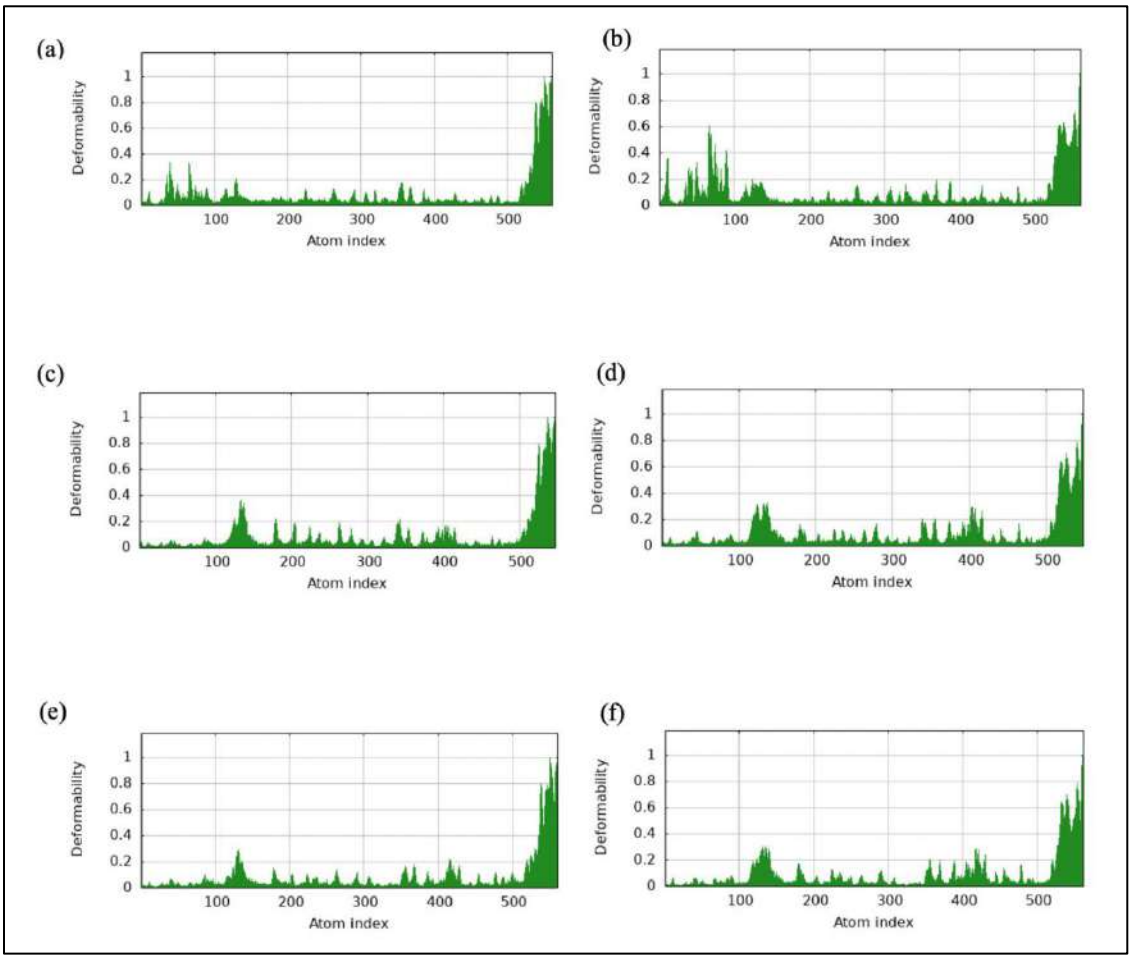

Figure 3. Deformability graph of the HADDOCK docked complexes (a) USP21 isoform a and YOD1 isoform 1 (b) USP21 isoform a and YOD1 isoform 2 (c) USP21 isoform b and YOD1 isoform 1 (d) USP21 isoform b and YOD1 isoform 2 (e) USP21 isoform c and YOD1 isoform 1 and (f) USP21 isoform c and YOD1 isoform 2.

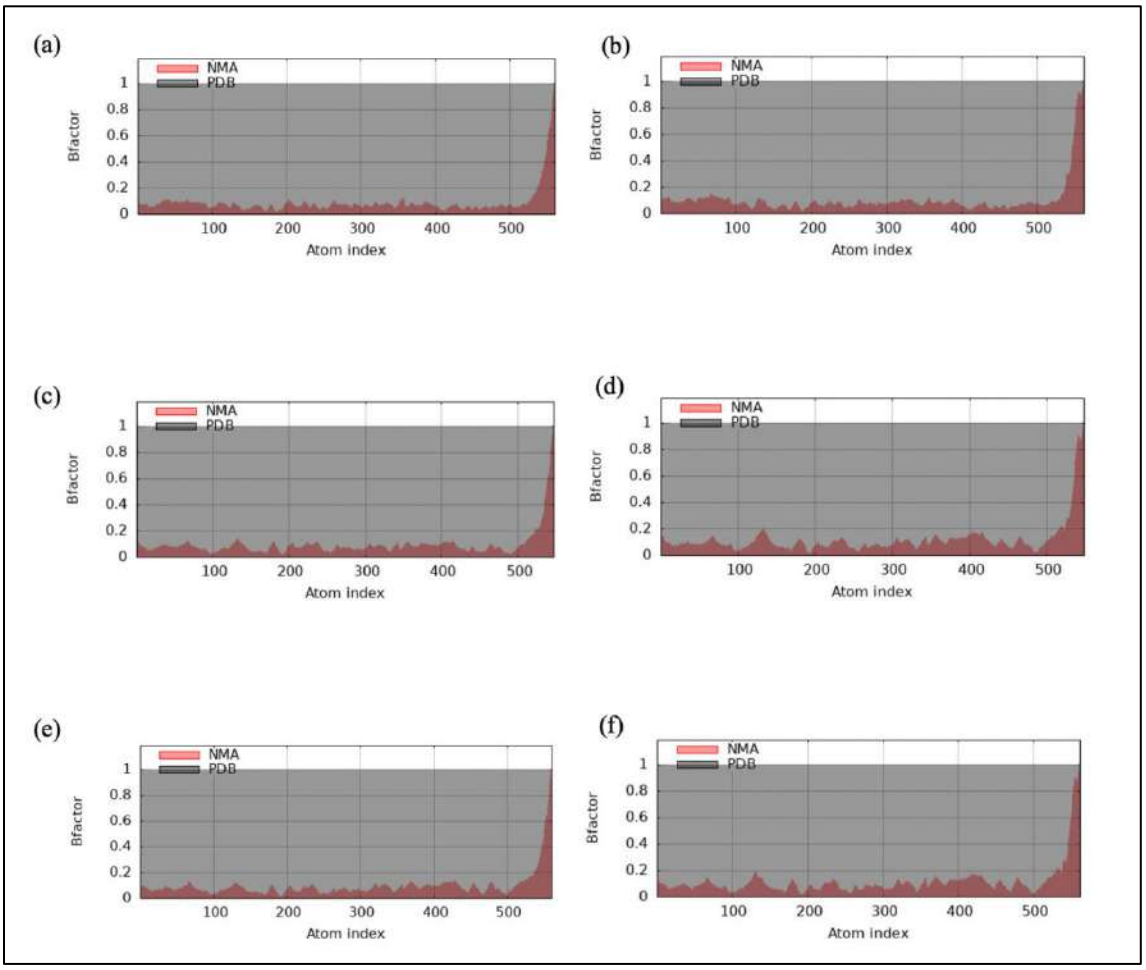

Figure 4. NMA calculation of the HADDOCK docked complexes (a) USP21 isoform a and YOD1 isoform 1 (b) USP21 isoform a and YOD1 isoform 2 (c) USP21 isoform b and YOD1 isoform 1 (d) USP21 isoform b and YOD1 isoform 2 (e) USP21 isoform c and YOD1 isoform 1 and (f) USP21 isoform c and YOD1 isoform 2.

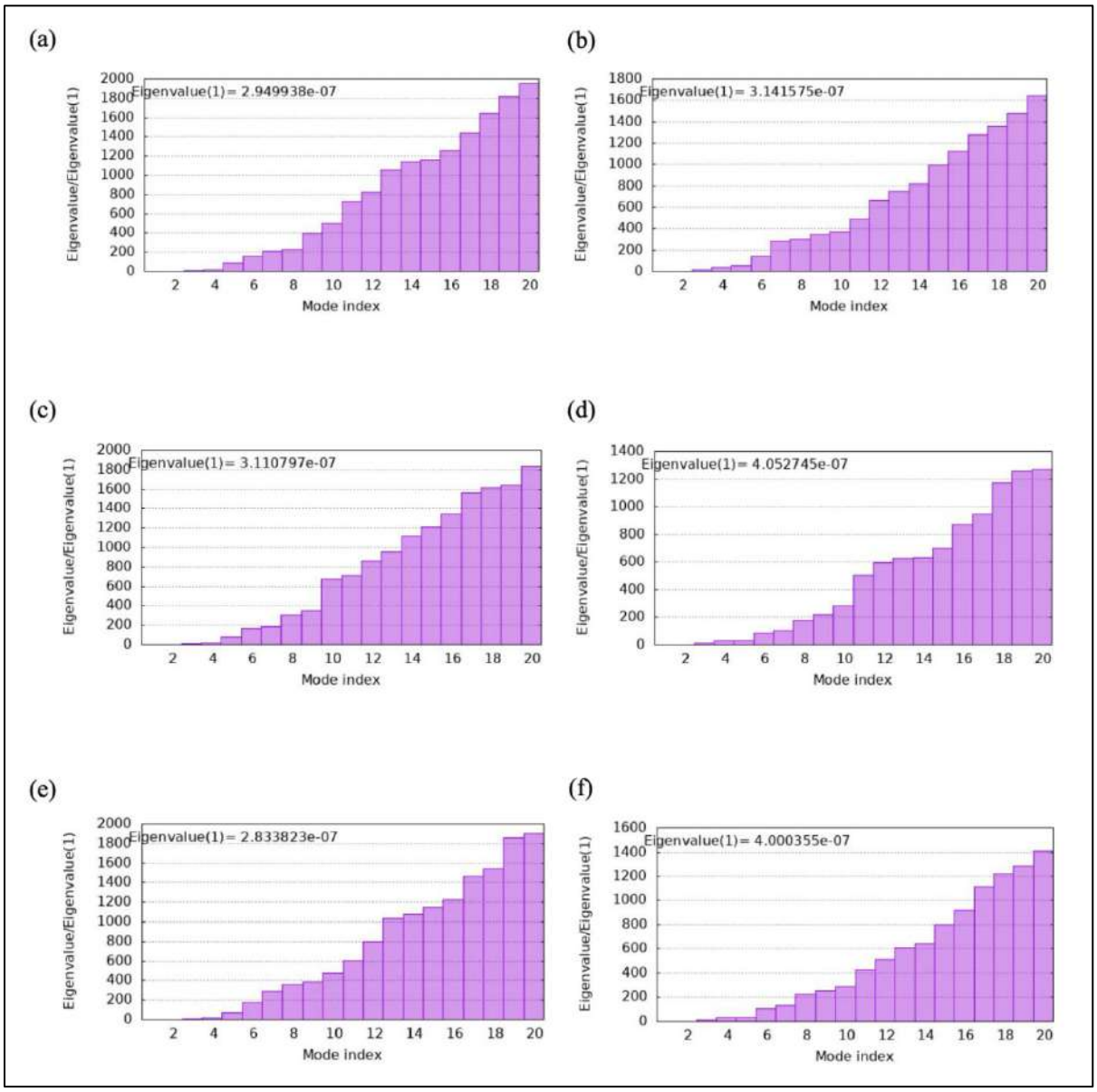

Figure 5. Eigenvalue of the HADDOCK docked complexes (a) USP21 isoform a and YOD1 isoform 1 (b) USP21 isoform a and YOD1 isoform 2 (c) USP21 isoform b and YOD1 isoform 1 (d) USP21 isoform b and YOD1 isoform 2 (e) USP21 isoform c and YOD1 isoform 1 and (f) USP21 isoform c and YOD1 isoform 2.

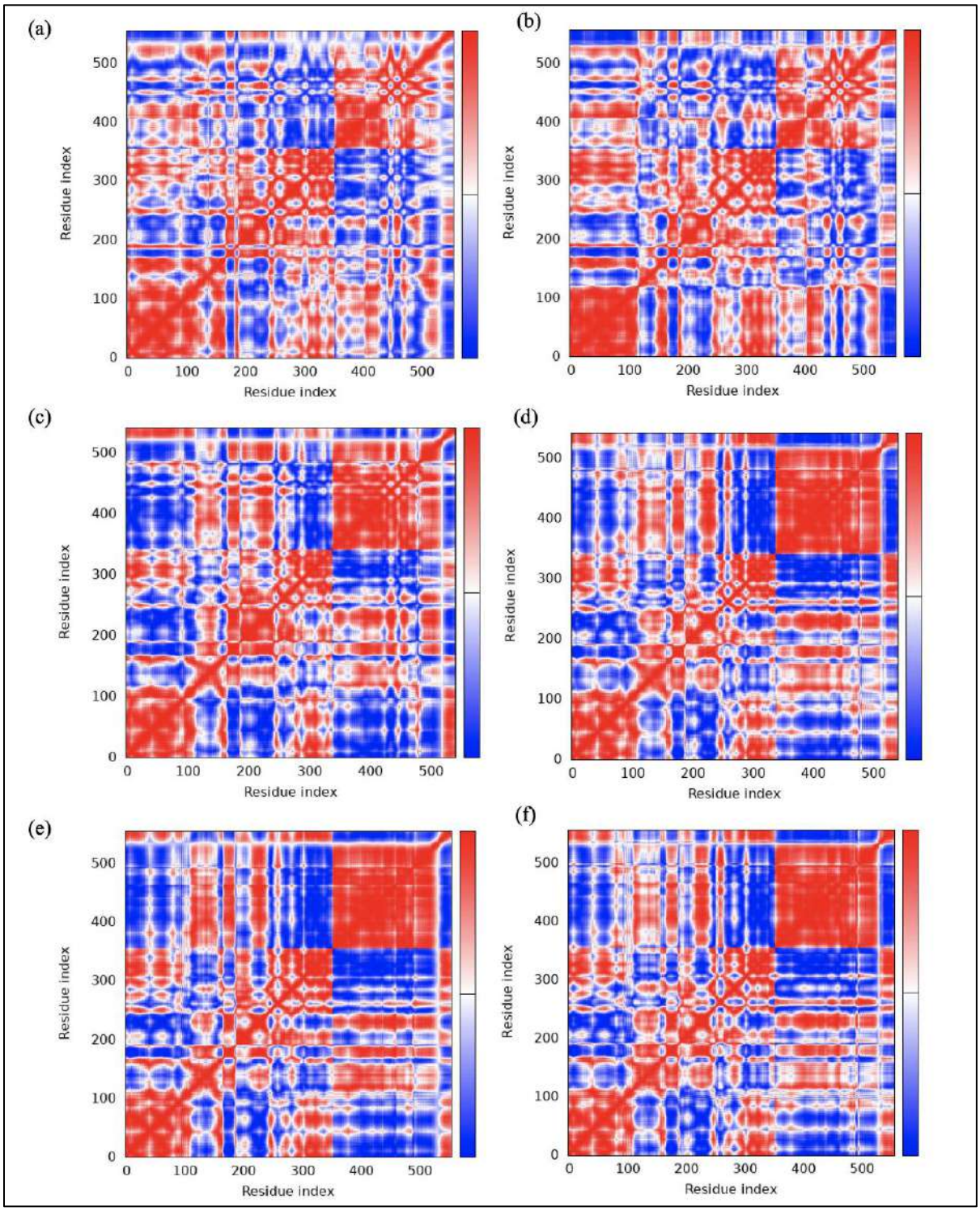

Figure 6. Covariance matrix of the HADDOCK docked complexes (a) USP21 isoform a and YOD1 isoform 1 (b) USP21 isoform a and YOD1 isoform 2 (c) USP21 isoform b and YOD1 isoform 1 (d) USP21 isoform b and YOD1 isoform 2 (e) USP21 isoform c and YOD1 isoform 1 and (f) USP21 isoform c and YOD1 isoform 2.

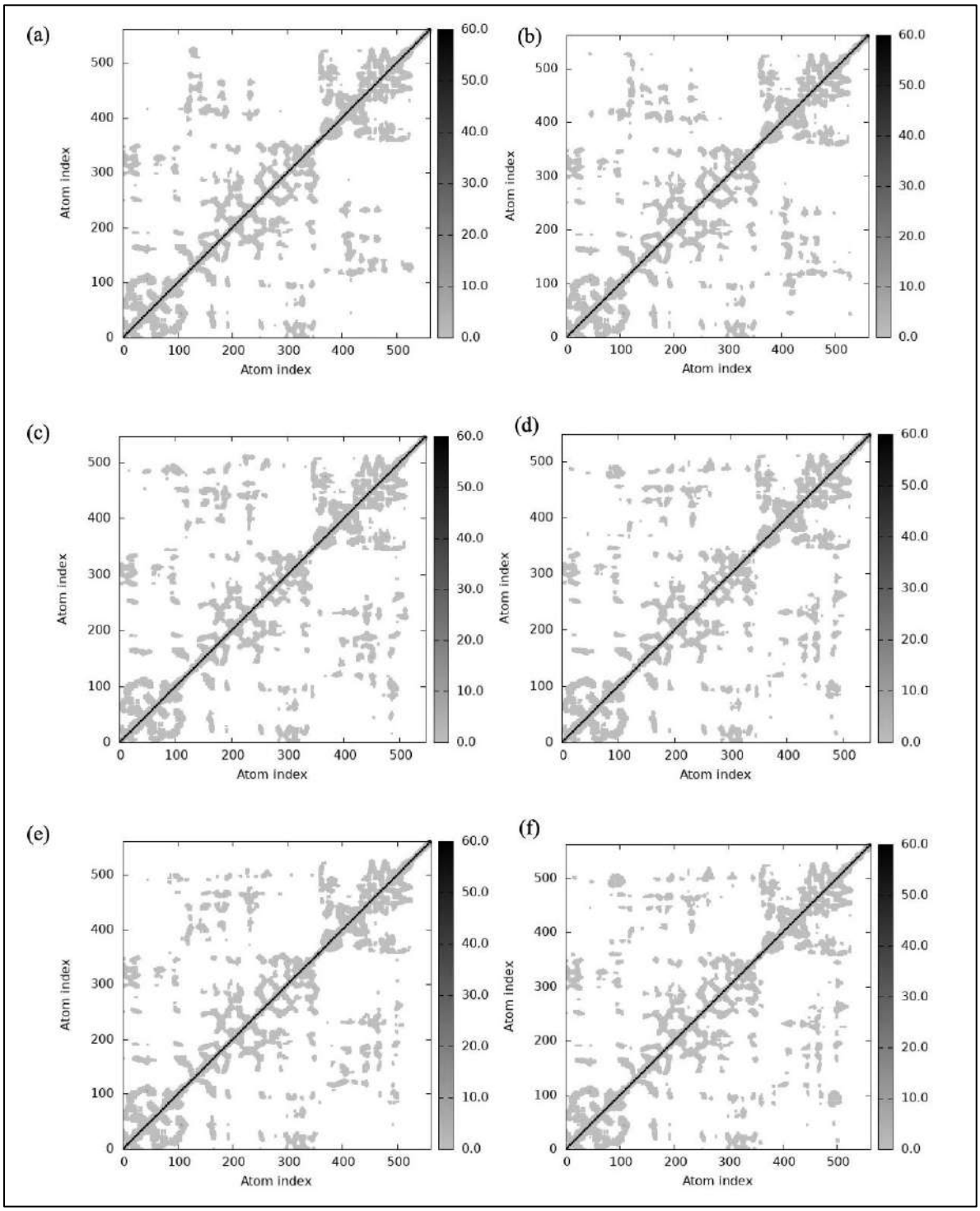

Figure 7. Elastic network models of the HADDOCK docked complexes (a) USP21 isoform a and YOD1 isoform 1 (b) USP21 isoform a and YOD1 isoform 2 (c) USP21 isoform b and YOD1 isoform 1 (d) USP21 isoform b and YOD1 isoform 2 (e) USP21 isoform c and YOD1 isoform 1 and (f) USP21 isoform c and YOD1 isoform 2.

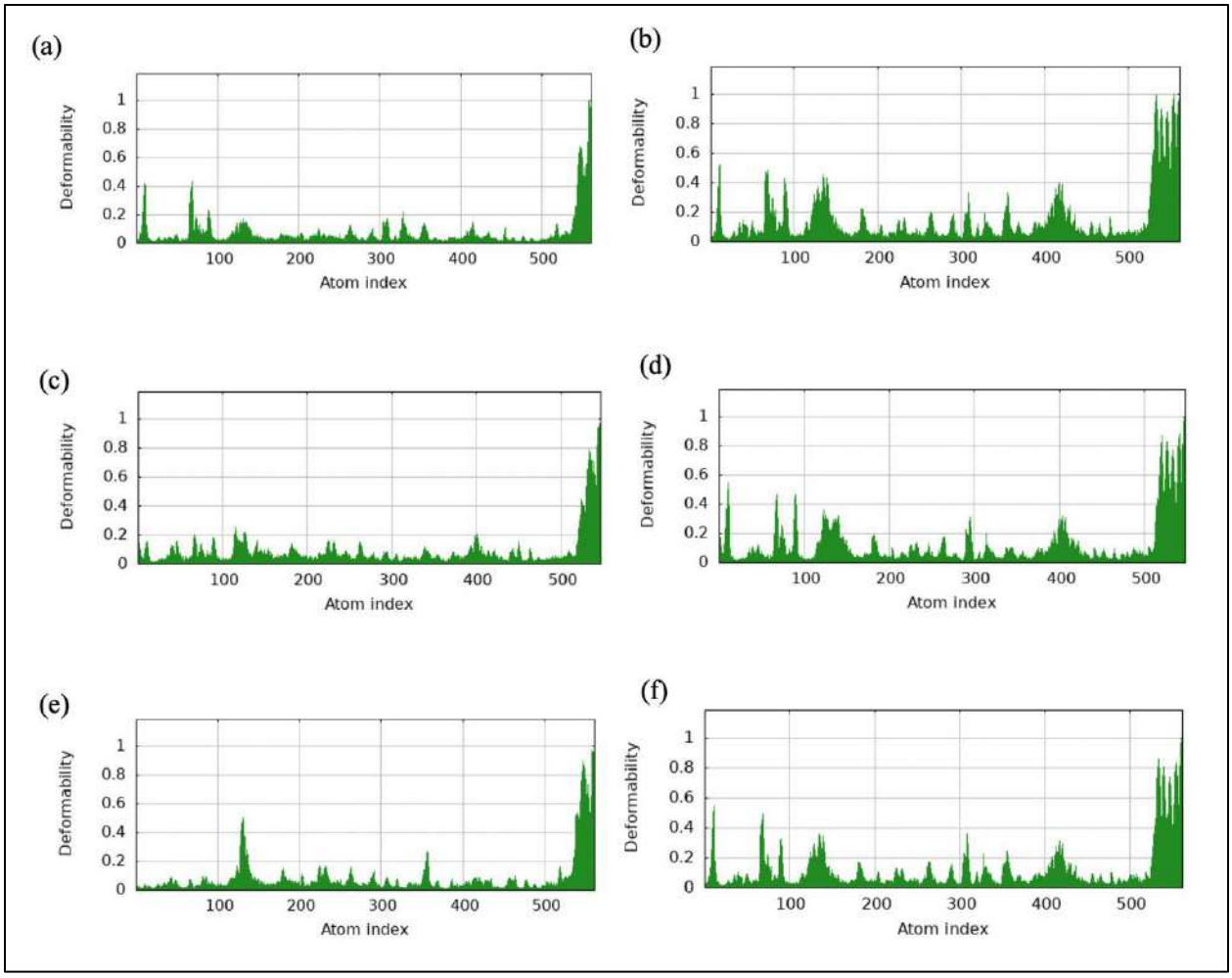

Figure 8. Deformability graph of the ClusPro docked complexes (a) USP21 isoform a and YOD1 isoform 1 (b) USP21 isoform a and YOD1 isoform 2 (c) USP21 isoform b and YOD1 isoform 1 (d) USP21 isoform b and YOD1 isoform 2 (e) USP21 isoform c and YOD1 isoform 1 and (f) USP21 isoform c and YOD1 isoform 2.

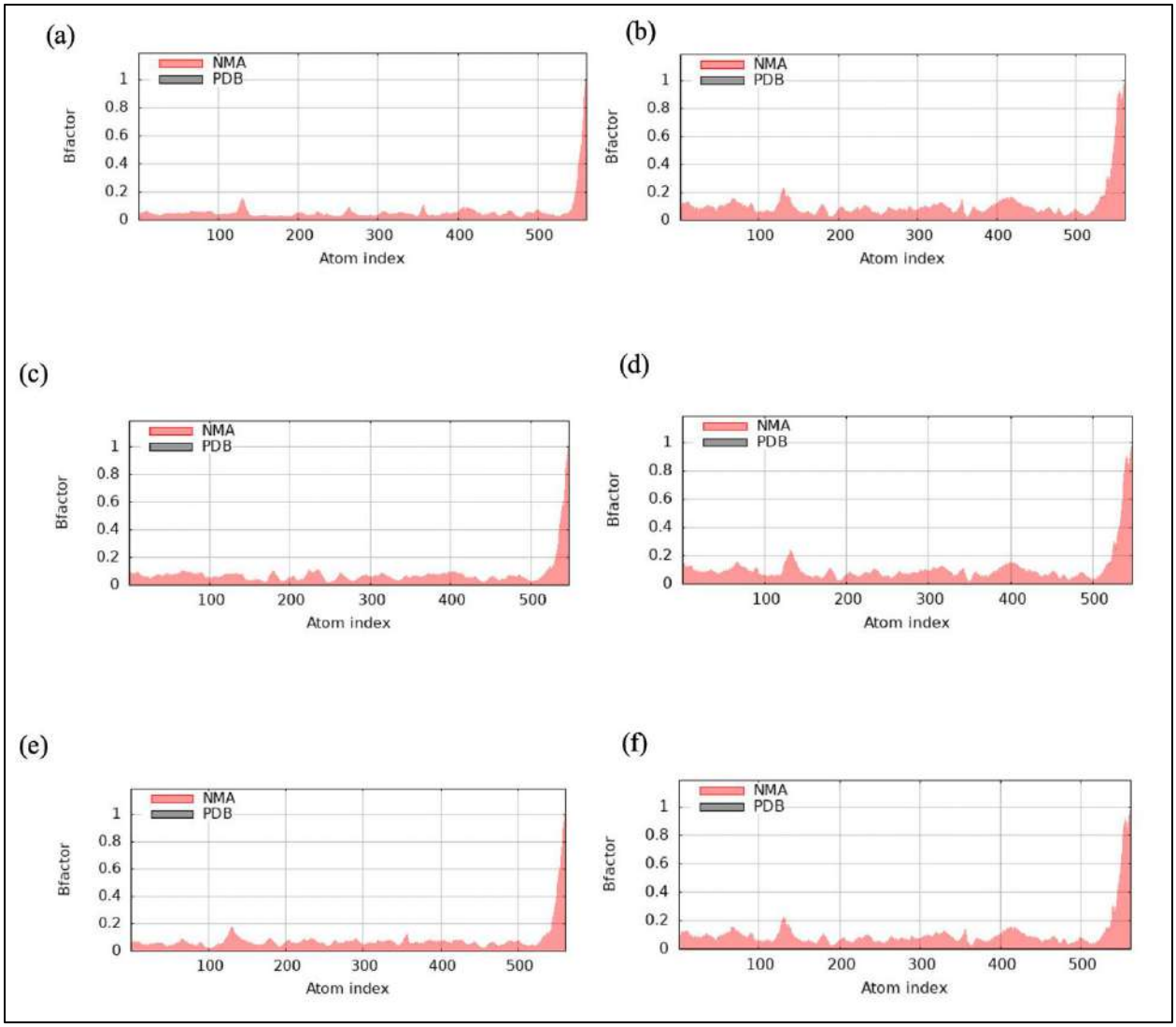

Figure 9. NMA calculation of the ClusPro docked complexes (a) USP21 isoform a and YOD1 isoform 1 (b) USP21 isoform a and YOD1 isoform 2 (c) USP21 isoform b and YOD1 isoform 1 (d) USP21 isoform b and YOD1 isoform 2 (e) USP21 isoform c and YOD1 isoform 1 and (f) USP21 isoform c and YOD1 isoform 2.

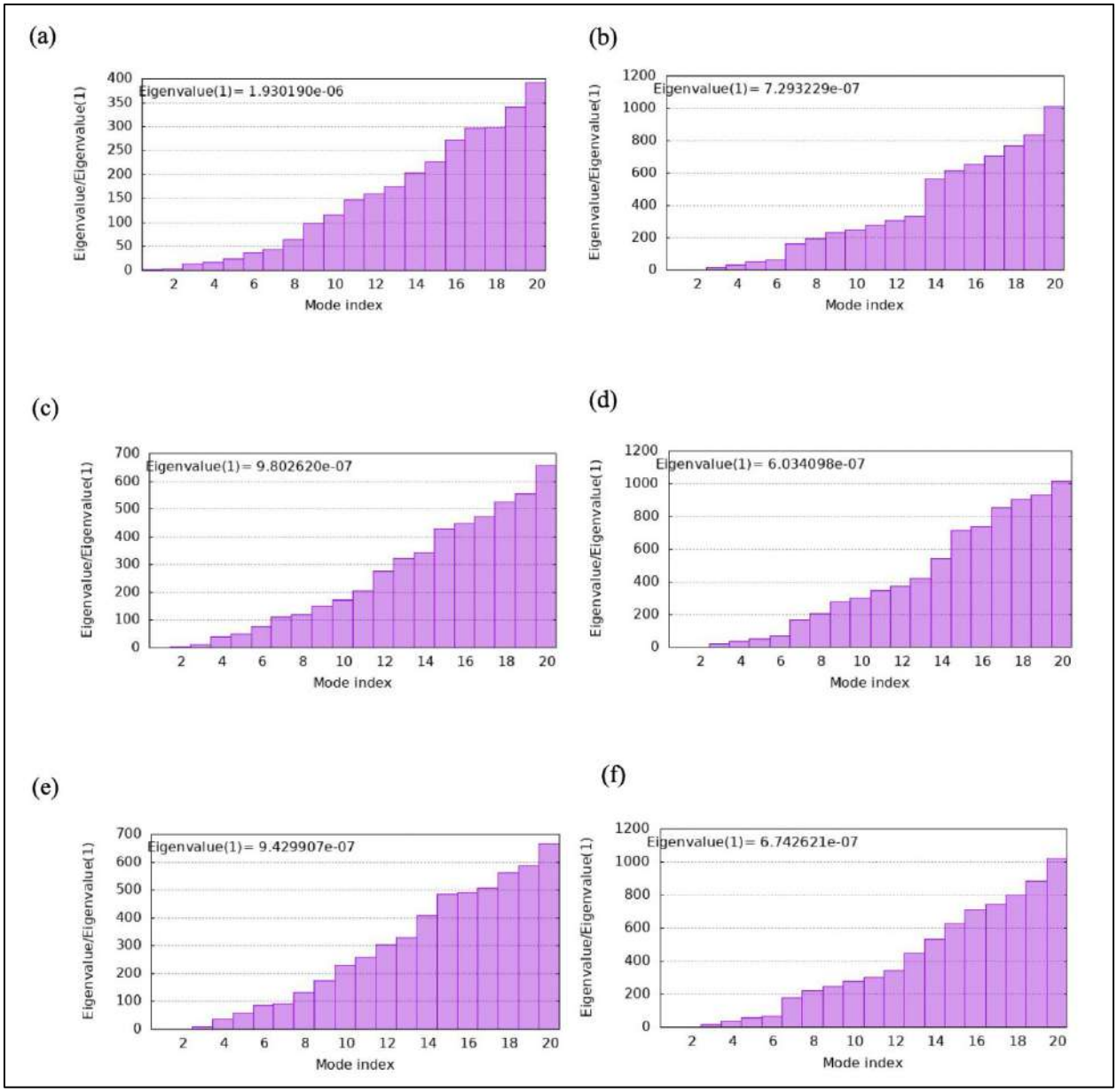

Figure 10. Eigenvalue of the ClusPro docked complexes (a) USP21 isoform a and YOD1 isoform 1 (b) USP21 isoform a and YOD1 isoform 2 (c) USP21 isoform b and YOD1 isoform 1 (d) USP21 isoform b and YOD1 isoform 2 (e) USP21 isoform c and YOD1 isoform 1 and (f) USP21 isoform c and YOD1 isoform 2.

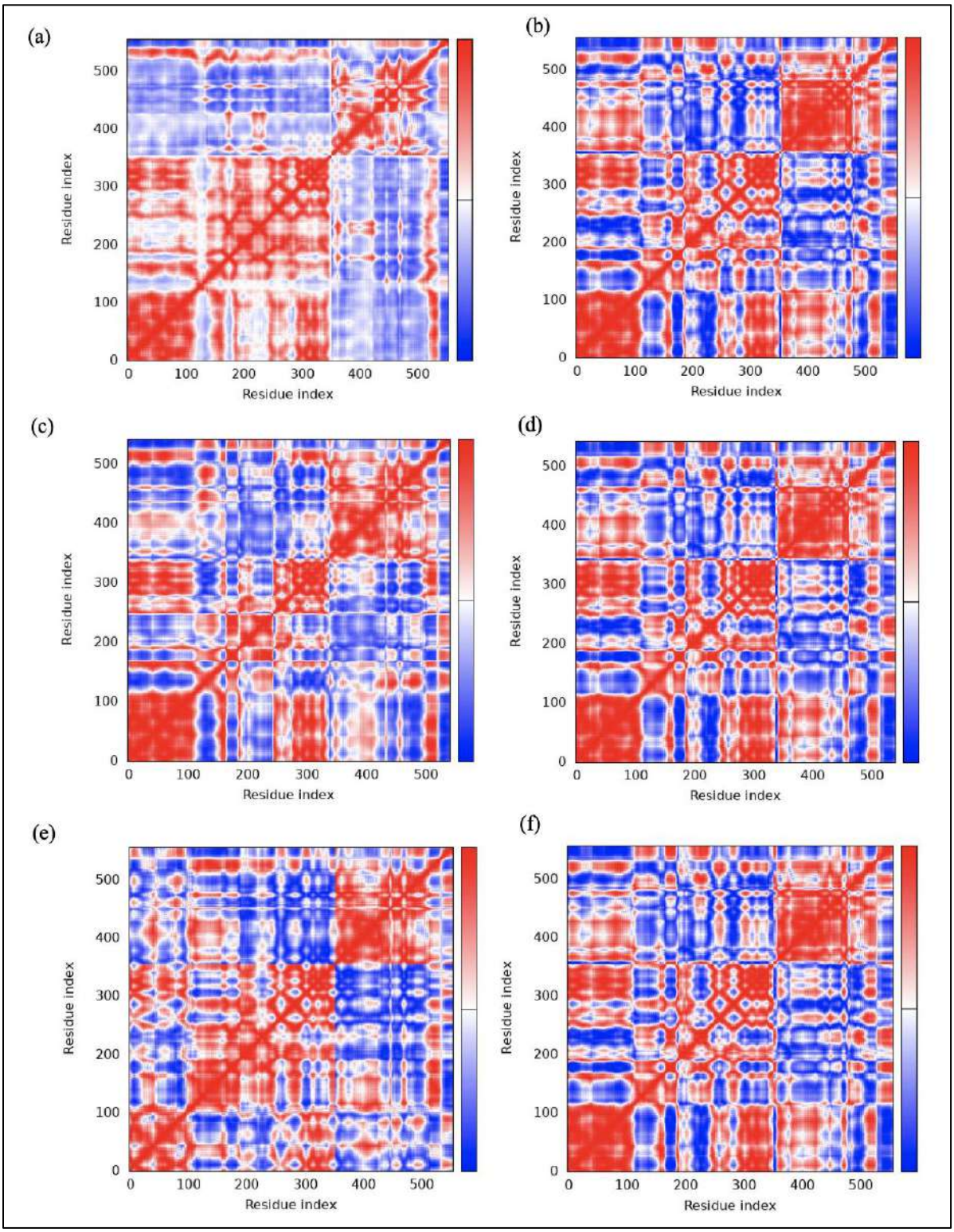

Figure 11. Covariance matrix of the ClusPro docked complexes (a) USP21 isoform a and YOD1 isoform 1 (b) USP21 isoform a and YOD1 isoform 2 (c) USP21 isoform b and YOD1 isoform 1 (d) USP21 isoform b and YOD1 isoform 2 (e) USP21 isoform c and YOD1 isoform 1 and (f) USP21 isoform c and YOD1 isoform 2.

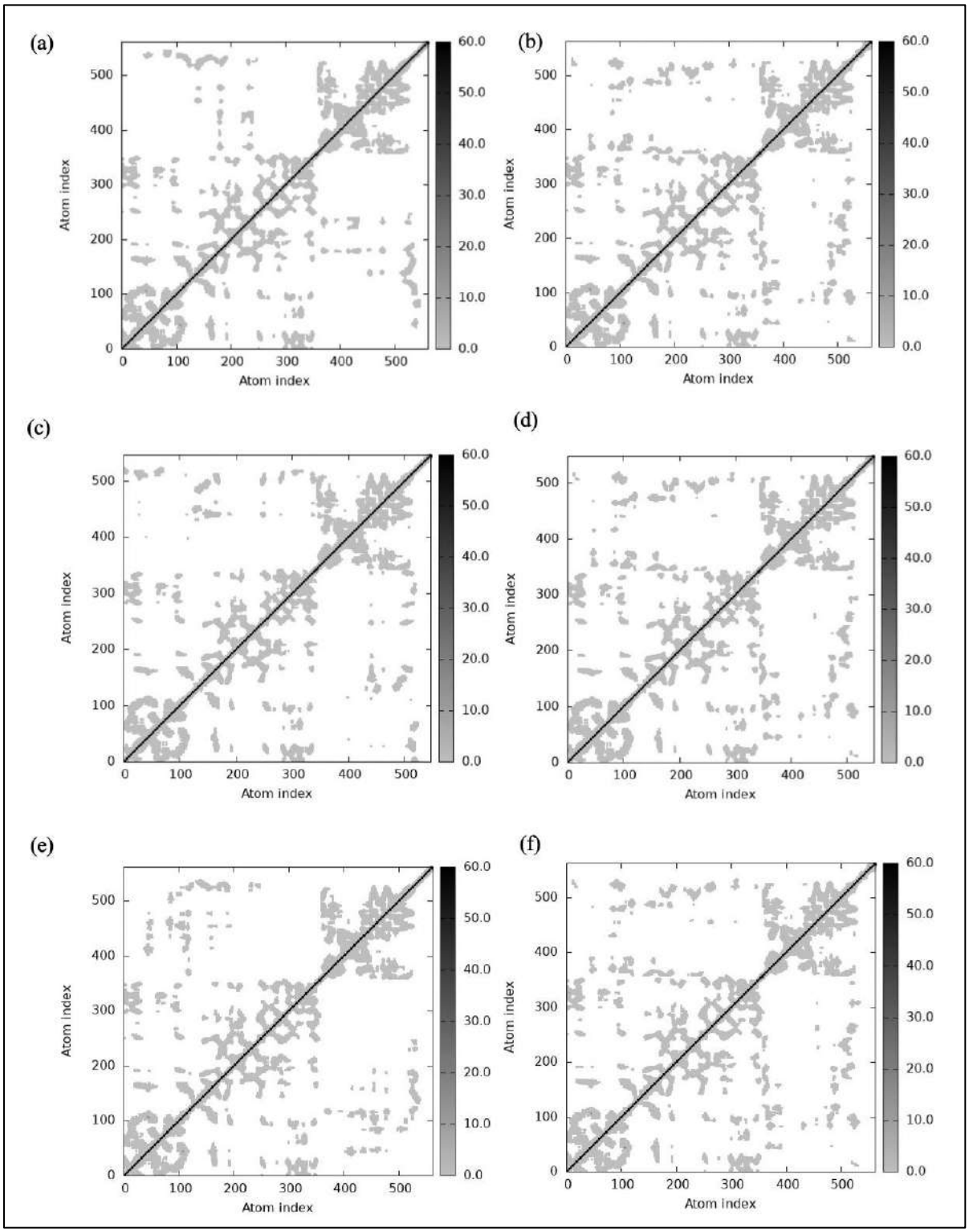

Figure 13. Elastic network models of the ClusPro docked complexes (a) USP21 isoform a and YOD1 isoform 1 (b) USP21 isoform a and YOD1 isoform 2 (c) USP21 isoform b and YOD1 isoform 1 (d) USP21 isoform b and YOD1 isoform 2 (e) USP21 isoform c and YOD1 isoform 1 and (f) USP21 isoform c and YOD1 isoform 2.

Discussion

The Hippo signalling pathway is essential for regulating cell proliferation during cancer development. The pathway's effector proteins, YAP and TAZ, are subject to continuous regulation. In the cytoplasm, ubiquitination is the primary mechanism for YAP/TAZ degradation. Deubiquitinating enzymes, including USP21 and YOD1, play significant roles in this process. In A549 cells, USP21 and YOD1 inhibit cell proliferation and demonstrate a synergistic effect (Park and Baek, 2023).

Multiple bioinformatics tools were employed to predict the interactions between isoforms of USP21 and YOD1. Protein sequences were retrieved in FASTA format from the NCBI protein database. Secondary structure predictions using the SIMPA96 toolkit provided insights into the isoform structures. The results indicated that all USP21 isoforms predominantly consist of random coils, with approximately 65% of residues forming random coils and about 25% forming alpha helices (Table 1). In comparison, YOD1 isoforms contained around 50% random coils and a similar proportion of alpha helices.

The three-dimensional structures of these proteins were designed using HHpred and several other tools to verify their accuracy. The total quality factor in the ERRAT value was above 85 for all proteins, which is within the acceptable range. However, USP21 isoform b had the highest ERRAT quality factor score among all the isoforms with a score of 92.46 (Table 2). More than 92% of residues of all proteins in the most favoured region are considered satisfactory values for the Ramachandran plot. The USP21 isoform showed the best score in terms of the Ramachandran plot, with almost 94.5% of residues in the Ramachandran favored regions (Table 2). The QMEANDisCo scores of all protein models were very near 0, which indicates high model quality. Interestingly, the QMEANDisCo scores of the isoforms of YOD1 were relatively lower than the scores of the isoforms of USP21.

Based on docking analysis, USP21 and YOD1 exhibit significant interactions with low binding energies. The ClusPro low-energy score showed that all docked complexes had scores below -1098.5, with the docked complex between USP21 isoform b and YOD1 isoform 2 having the lowest score of -1321.21. However, docking in HADDOCK showed different results. In HADDOCK, the docked complexes of USP21 isoform b and YOD1 isoform 1 exhibited a score of 57.4 ± 1.9. The Z-score of this docked complex was also quite low at -1.8, which was close to the lowest score of -1.9 of docking between USP21 isoform c and YOD1 isoform 1 (Table 3). Analysis of the docked complexes in BIOVIA Discovery Studio demonstrated that all complexes exhibited extensive binding, with hydrogen bonds, alkyl interactions, and salt bridges being the most common types of interactions. PRODIGY was used to determine the binding affinity of the selected protein isoforms. Although the binding affinity of all docked complexes was low, the binding affinity between USP21 isoform b and YOD1 isoform 1 was predicted the lowest at -18.3 kcal/mol (Table 3).

In molecular dynamics simulation studies with HADDOCK results, almost all docked complexes showed good stability, which was confirmed by deformability, *B*-factor, eigenvalues, covariance maps and elastic network graphs (Figure 04-08). Most of the docked complexes showed similar spikes in the deformability graph and the B-factor graph (Figure 04 and 05). The Eigenvalue of all complexes seems to be in a close range (Figure 06). The covariance matrix and elastic network models of all docked complexes also show a similar picture (Figures 07 and 08). However, if we consider molecular dynamics simulation studies with ClusPro results, we can see that the docking between USP21 isoform b and YOD1 isoform 1 is the most stable among all (Figure 09-13). It shows the best results in the deformability graph, with very few spikes for atoms (Figure 09). The NMA calculation graph also does not exhibit any significant peaks throughout the graph (Figure 10). The covariance matrix and elastic network models also show the best stability of this complex, with most atoms remaining in the central grey area, while other graphs show more scattered results (Figures 12-13).

Considering both the docking and simulation results, it can be concluded that the binding between USP21 isoform b and YOD1 isoform 1 seems more stable and easier to form. Since these two proteins were discovered to interact with each other, and this interaction results in better degradation of YAP/TAZ to inhibit Hippo signaling pathway-mediated cell proliferation in A549 cells, it can be predicted that the binding between USP21 isoform b and YOD1 isoform 1 has a better chance of suppressing lung cancer than other isoforms.

Conclusion

This study was designed to identify which set of isoforms of USP21 and YOD1 interact most effectively and what this means for lung cancer. It would be beneficial to study the specific mechanisms by which these two enzymes interact for a better understanding of lung cancer's molecular basis. Targeting these enzymes may also present novel therapeutic options, which may result in personalized and efficient treatment strategies. Future studies should clarify the complex interactions between these enzymes and investigate their potential as therapeutic targets to improve clinical outcomes for lung cancer patients.

Funding Statement

There was no funding for the research and publication of this article.

Competing Interests

The authors declare no competing interests.

Availability of Data and Material

All the data presented in this manuscript are available on request to the corresponding author.

Declaration of AI assistance in Manuscript Preparation

During the preparation of this manuscript the author(s) used ChatGPT in order to improve the language of the manuscript. After using this tool, the author(s) reviewed and edited the content as needed and take(s) full responsibility for the content of the publication.

References

1. Austin, K.M., Trembley, M.A., Chandler, S.F., Sanders, S.P., Saffitz, J.E., Abrams, D.J. and Pu, W.T. (2019), *Molecular Mechanisms of Arrhythmogenic Cardiomyopathy*, *Nature Reviews Cardiology*, Vol. 16, available at:https://doi.org/10.1038/s41569-019-0200-7.

2. Balakirev, M.Y., Tcherniuk, S.O., Jaquinod, M. and Chroboczek, J. (2003), "Otubains: A new family of cysteine proteases in the ubiquitin pathway", *EMBO Reports*, Vol. 4 No. 5, pp. 517–522.

3. Benkert, P., Tosatto, S.C.E. and Schomburg, D. (2008), "QMEAN: A comprehensive scoring function for model quality assessment", *Proteins: Structure, Function and Genetics*, Vol. 71 No. 1, pp. 261–277.
4. Bergmann, C., Guay-Woodford, L.M., Harris, P.C., Horie, S., Peters, D.J.M. and Torres, V.E. (2018), "Polycystic kidney disease", *Nature Reviews Disease Primers*, Vol. 4 No. 1, p. 50.
5. Chan, E.H.Y., Nousiainen, M., Chalamalasetty, R.B., Schäfer, A., Nigg, E.A. and Sillje, H.H.W. (2005), "The Ste20-like kinase Mst2 activates the human large tumor suppressor kinase Lats1", *Oncogene*, Vol. 24 No. 12, pp. 2076–2086.
6. Chanda, D., Otoupalova, E., Smith, S.R., Volckaert, T., De Langhe, S.P. and Thannickal, V.J. (2019), "Developmental pathways in the pathogenesis of lung fibrosis", *Molecular Aspects of Medicine*, Vol. 65 No. 205, pp. 56–69.
7. Chen, Z.J. and Sun, L.J. (2009), "Nonproteolytic Functions of Ubiquitin in Cell Signaling", *Molecular Cell*, Elsevier Inc., Vol. 33 No. 3, pp. 275–286.
8. Cheng, J., Wang, S., Dong, Y. and Yuan, Z. (2020), "The Role and Regulatory Mechanism of Hippo Signaling Components in the Neuronal System", *Frontiers in Immunology*, Vol. 11 No. February, pp. 1–7.
9. Clague, M.J., Coulson, J.M. and Urbé, S. (2012), "Cellular functions of the DUBs", *Journal of Cell Science*, Vol. 125 No. 2, pp. 277–286.
10. Colovos, C. and Yeates, T.O. (1993), "Verification of protein structures: Patterns of nonbonded atomic interactions", *Protein Science*, Vol. 2 No. 9, pp. 1511–1519.
11. Driskill, J.H. and Pan, D. (2021), "The Hippo Pathway in Liver Homeostasis and Pathophysiology", *Annual Review of Pathology: Mechanisms of Disease*, Vol. 16 No. 1, pp. 299–322.
12. Ernst, R., Mueller, B., Ploegh, H.L. and Schlieker, C. (2009), "7The Otubain YOD1 Is a Deubiquitinating Enzyme that Associates with p97 to Facilitate Protein Dislocation from the ER", *Molecular Cell*, Elsevier Ltd, Vol. 36 No. 1, pp. 28–38.
13. Gröhl, J., Dreher, K.K., Schellenberg, M., Rix, T., Holzwarth, N., Vieten, P., Ayala, L., *et al.* (2022), "SIMPA: an open-source toolkit for simulation and image processing for photonics and acoustics", *Journal of Biomedical Optics*, Vol. 27 No. 08, pp. 1–21.
14. Hall, C.A., Wang, R., Miao, J., Oliva, E., Shen, X., Wheeler, T., Hilsenbeck, S.G., *et al.* (2010), "Hippo pathway effector Yap is an ovarian cancer oncogene", *Cancer Research*, Vol. 70 No. 21, pp. 8517–8525.
15. Heo, L., Park, H. and Seok, C. (2013), "GalaxyRefine: Protein structure refinement driven by side-chain repacking.", *Nucleic Acids Research*, Vol. 41 No. Web Server issue, pp. 384–388.
16. Hergovich, A., Schmitz, D. and Hemmings, B.A. (2006), "The human tumour suppressor LATS1 is activated by human MOB1 at the membrane", *Biochemical and Biophysical Research Communications*, Vol. 345 No. 1, pp. 50–58.
17. Hong, L., Li, X., Zhou, D., Geng, J. and Chen, L. (2018), "Role of Hippo signaling in regulating immunity", *Cellular and Molecular Immunology*, Springer US, Vol. 15 No. 12, pp. 1003–1009.
18. Honorato, R. V., Trellet, M.E., Jiménez-García, B., Schaarschmidt, J.J., Giulini, M., Reys, V., Koukos, P.I., *et al.* (2024), *The HADDOCK2.4 Web Server for Integrative Modeling of Biomolecular Complexes*, *Nature Protocols*, Vol. 19, available at:https://doi.org/10.1038/s41596-024-01011-0.
19. Huang, J., Wu, S., Barrera, J., Matthews, K. and Pan, D. (2005), "The Hippo signaling pathway coordinately regulates cell proliferation and apoptosis by inactivating Yorkie, the Drosophila homolog of YAP", *Cell*, Vol. 122 No. 3, pp. 421–434.
20. Kemmish, H., Fasnacht, M. and Yan, L. (2017), "Fully automated antibody structure prediction using BIOVIA tools: Validation study", *PLoS ONE*, Vol. 12 No. 5, pp. 1–26.
21. Kozakov, D., Hall, D.R., Xia, B., Porter, K.A., Padhorny, D., Yueh, C., Beglov, D., *et al.* (2017), "84. The ClusPro web server for protein–protein docking", *Nature Protocols*, Vol. 12 No. 2, pp. 255–278.
22. Kwon, Y., Vinayagam, A., Sun, X., Dephoure, N., Gygi, S.P., Hong, P. and Perrimon, N. (2013), "The Hippo signaling pathway interactome", *Science*, Vol. 342 No. 6159, pp. 737–740.
23. Laskowski, R.A., MacArthur, M.W., Moss, D.S. and Thornton, J.M. (1993), "PROCHECK: a program to check the stereochemical quality of protein structures", *Journal of Applied Crystallography*, International Union of Crystallography, Vol. 26 No. 2, pp. 283–291.
24. Lee, M., Goraya, N., Kim, S. and Cho, S.H. (2018), "Hippo-yap signaling in ocular development and disease", *Developmental Dynamics*, Vol. 247 No. 6, pp. 794–806.
25. Li, Z., Liu, X., Yu, H., Wang, S., Zhao, S. and Jiang, G. (2022), "62. USP21 regulates Hippo signaling to promote radioresistance by deubiquitinating FOXM1 in cervical cancer", *Human Cell*, Springer Singapore, Vol. 35 No. 1, pp. 333–347.
26. Liu, C.-Y., Zha, Z.-Y., Zhou, X., Zhang, H., Huang, W., Zhao, D., Li, T., *et al.* (2010), "The Hippo Tumor Pathway Promotes TAZ Degradation by Phosphorylating a Phosphodegron and Recruiting the SCFβ-TrCP E3 Ligase", *Journal of Biological Chemistry*, Vol. 285 No. 48, pp. 37159–37169.
27. López-Blanco, J.R., Aliaga, J.I., Quintana-Ortí, E.S. and Chacón, P. (2014), "88. IMODS: Internal coordinates normal mode analysis server", *Nucleic Acids Research*, Vol. 42 No. W1, pp. 271–276.
28. Lu, L., Li, Y., Kim, S.M., Bossuyt, W., Liu, P., Qiu, Q., Wang, Y., *et al.* (2010), "Hippo signaling is a potent in vivo growth and tumor suppressor pathway in the mammalian liver", *Proceedings of the National Academy of Sciences of the United States of America*, Vol. 107 No. 4, pp. 1437–1442.
29. Ma, S. and Guan, K.L. (2018), "Polycystic kidney disease: A Hippo connection", *Genes and Development*, Vol. 32 No. 11–12, pp. 737–739.
30. Makarova, K.S., Aravind, L. and Koonin, E. V. (2000), "A novel superfamily of predicted cysteine proteases from eukaryotes, viruses and Chlamydia pneumoniae", *Trends in Biochemical Sciences*, Vol. 25 No. 2, pp. 50–52.
31. Nguyen, H.T., Kugler, J.M., Loya, A.C. and Cohen, S.M. (2017), "USP21 regulates Hippo pathway activity by mediating MARK protein turnover", *Oncotarget*, Vol. 8 No. 38, pp. 64095–64105.
32. Nijman, S.M.B., Huang, T.T., Dirac, A.M.G., Brummelkamp, T.R., Kerkhoven, R.M., D'Andrea, A.D. and Bernards, R. (2005), "The deubiquitinating enzyme USP1 regulates the fanconi anemia pathway", *Molecular Cell*, Vol. 17 No. 3, pp. 331–339.
33. Papadopoulos, C., Kirchner, P., Bug, M., Grum, D., Koerver, L., Schulze, N., Poehler, R., *et al.* (2017), "VCP/p97 cooperates with YOD1, UBXD1 and PLAA to drive clearance of ruptured

lysosomes by autophagy", *The EMBO Journal*, Vol. 36 No. 2, pp. 135–150.
34. Park, S.S. and Baek, K.H. (2023), "74. Synergistic effect of YOD1 and USP21 on the Hippo signaling pathway", *Cancer Cell International*, BioMed Central, Vol. 23 No. 1, pp. 1–13.
35. Praskova, M., Xia, F. and Avruch, J. (2008), "MOBKL1A/MOBKL1B Phosphorylation by MST1 and MST2 Inhibits Cell Proliferation", *Current Biology*, Vol. 18 No. 5, pp. 311–321.
36. Qin, X., Lv, X., Li, P., Yang, R., Xia, Q., Chen, Y., Peng, Y., *et al.* (2020), "Matrix stiffness modulates ILK-mediated YAP activation to control the drug resistance of breast cancer cells", *Biochimica et Biophysica Acta - Molecular Basis of Disease*, Vol. 1866 No. 3, available at: https://doi.org/10.1016/j.bbadis.2019.165625.
37. Ren, A., Yan, G., You, B. and Sun, J. (2008), "Down-regulation of mammalian sterile 20-like kinase 1 by heat shock protein 70 mediates cisplatin resistance in prostate cancer cells", *Cancer Research*, Vol. 68 No. 7, pp. 2266–2274.
38. Reyes-Turcu, F.E., Ventii, K.H. and Wilkinson, K.D. (2009), "Regulation and Cellular Roles of Ubiquitin-Specific Deubiquitinating Enzymes", *Annual Review of Biochemistry*, Vol. 78 No. 1, pp. 363–397.
39. Rodesch, C., Geyer, P.K., Patton, J.S., Bae, E. and Nagoshi, R.N. (1995), "Developmental analysis of the ovarian tumor gene during Drosophila oogenesis", *Genetics*, Vol. 141 No. 1, pp. 191–202.
40. Russell, J.O. and Camargo, F.D. (2022), "Hippo signalling in the liver: role in development, regeneration and disease", *Nature Reviews Gastroenterology and Hepatology*, Vol. 19 No. 5, pp. 297–312.
41. Sass, G.L., Comer, A.R. and Searles, L.L. (1995), "The Ovarian Tumor Protein Isoforms of Drosophila melanogaster Exhibit Differences in Function, Expression, and Localization", *Developmental Biology*, Vol. 167 No. 1, pp. 201–212.
42. Sayers, E.W., Barrett, T., Benson, D.A., Bolton, E., Bryant, S.H., Canese, K., Chetvernin, V., *et al.* (2011), "Database resources of the national center for biotechnology information", *Nucleic Acids Research*, Vol. 39 No. SUPPL. 1, pp. 38–51.
43. Söding, J., Biegert, A. and Lupas, A.N. (2005), "The HHpred interactive server for protein homology detection and structure prediction", *Nucleic Acids Research*, Vol. 33 No. SUPPL. 2, pp. 244–248.
44. Sun, H.L., Men, J.R., Liu, H.Y., Liu, M.Y. and Zhang, H.S. (2020), "FOXM1 facilitates breast cancer cell stemness and migration in YAP1-dependent manner", *Archives of Biochemistry and Biophysics*, Elsevier, Vol. 685 No. January, p. 108349.
45. Touil, Y., Igoudjil, W., Corvaisier, M., Dessein, A.F., Vandomme, J., Monte, D., Stechly, L., *et al.* (2014), "Colon cancer cells escape 5FU chemotherapy-induced cell death by entering stemness and quiescence associated with the c-Yes/YAP axis", *Clinical Cancer Research*, Vol. 20 No. 4, pp. 837–846.
46. Wang, J., Liu, S., Heallen, T. and Martin, J.F. (2018), "The Hippo pathway in the heart: pivotal roles in development, disease, and regeneration", *Nature Reviews Cardiology*, Springer US, Vol. 15 No. 11, pp. 672–684.
47. Wang, X., Sun, D., Tai, J., Chen, S., Yu, M., Ren, D. and Wang, L. (2018), "TFAP2C promotes stemness and chemotherapeutic resistance in colorectal cancer via inactivating hippo signaling pathway", *Journal of Experimental and Clinical Cancer Research*, Journal of Experimental and Clinical Cancer Research, Vol. 37 No. 1, pp. 1–16.
48. Wu, Q., Guo, J., Liu, Y., Zheng, Q., Li, X., Wu, C., Fang, D., *et al.* (2021), "YAP drives fate conversion and chemoresistance of small cell lung cancer", *Science Advances*, Vol. 7 No. 40, pp. 1–20.
49. Xia, H., Qi, H., Li, Y., Pei, J., Barton, J., Blackstad, M., Xu, T., *et al.* (2002), "LATS1 tumor suppressor regulates G2/M transition and apoptosis", *Oncogene*, Vol. 21 No. 8, pp. 1233–1241.
50. Xu, P., Xiao, H., Yang, Q., Hu, R., Jiang, L., Bi, R., Jiang, X., *et al.* (2020), "The USP21/YY1/SNHG16 axis contributes to tumor proliferation, migration, and invasion of non-small-cell lung cancer", *Experimental and Molecular Medicine*, Springer US, Vol. 52 No. 1, pp. 41–55.
51. Xue, L.C., Rodrigues, J.P., Kastritis, P.L., Bonvin, A.M. and Vangone, A. (2016), "PRODIGY: A web server for predicting the binding affinity of protein-protein complexes", *Bioinformatics*, Vol. 32 No. 23, pp. 3676–3678.
52. Yao, W., Zhu, S., Li, P. and Zhang, S. (2019), "Large tumor suppressor kinase 2 overexpression attenuates 5-FU-resistance in colorectal cancer via activating the JNK-MIEF1-mitochondrial division pathway", *Cancer Cell International*, BioMed Central, Vol. 19 No. 1, pp. 1–15.
53. Zeng, R. and Dong, J. (2021), "The hippo signaling pathway in drug resistance in cancer", *Cancers*, Vol. 13 No. 2, pp. 1–23.
54. Zhang, X., George, J., Deb, S., Degoutin, J.L., Takano, E.A., Fox, S.B., Bowtell, D.D.L., *et al.* (2011), "The Hippo pathway transcriptional co-activator, YAP, is an ovarian cancer oncogene", *Oncogene*, Nature Publishing Group, Vol. 30 No. 25, pp. 2810–2822.
55. Zhang, Y., Zhang, H. and Zhao, B. (2018), "Hippo Signaling in the Immune System", *Trends in Biochemical Sciences*, Elsevier Ltd, Vol. 43 No. 2, pp. 77–80.
56. Zhao, B., Li, L., Tumaneng, K., Wang, C.-Y. and Guan, K.-L. (2010), "A coordinated phosphorylation by Lats and CK1 regulates YAP stability through SCF β-TRCP", *Genes and Development*, Vol. 24 No. 1, pp. 72–85.
57. Zhao, B., Wei, X., Li, W., Udan, R.S., Yang, Q., Kim, J., Xie, J., *et al.* (2007), "Inactivation of YAP oncoprotein by the Hippo pathway is involved in cell contact inhibition and tissue growth control", *Genes and Development*, Vol. 21 No. 21, pp. 2747–2761.
58. Zhou, D., Conrad, C., Xia, F., Park, J.S., Payer, B., Yin, Y., Lauwers, G.Y., *et al.* (2009), "Mst1 and Mst2 Maintain Hepatocyte Quiescence and Suppress Hepatocellular Carcinoma Development through Inactivation of the Yap1 Oncogene", *Cancer Cell*, Elsevier Ltd, Vol. 16 No. 5, pp. 425–438.
59. Zhu, J.Y., Lin, S. and Ye, J. (2018), "YAP and TAZ, the conductors that orchestrate eye development, homeostasis, and disease", *Journal of Cellular Physiology*, Vol. 234 No. 1, pp. 246–258.
60. Zimmermann, L., Stephens, A., Nam, S.-Z., Rau, D., Kübler, J., Lozajic, M., Gabler, F., *et al.* (2018), "A Completely Reimplemented MPI Bioinformatics Toolkit with a New HHpred Server at its Core", *Journal of Molecular Biology*, Vol. 430 No. 15, pp. 2237–2243.